On the detection of marine mammals with ship-borne polarimetric microwave radar

S. J. Anderson and J.T. Morris
Defence Science and Technology Organisation
PO Box 1500
Edinburgh SA 5111 Australia

Abstract- **Collisions between ships and whales are not rare occurrences. Apart from constituting a major cause of death for whale species which frequent busy oceanic areas such as the North Atlantic, such collisions often result in damage to ships. Thus there is keen interest in finding reliable means of detection of whales at sufficient range to ensure successful collision avoidance. In this paper we present the results of experiments aimed at establishing the potential of polarimetric microwave radar to provide such a means. The key element in our approach is the construction of a polarimetric filter which enhances the contrast between the disturbed sea surface around the whale and the ambient sea. The results suggest that detection can be achieved under conditions where conventional uni-polar radars such as those normally found on merchant ships would fail.**

I. INTRODUCTION

It might be thought that the probability of a ship colliding with a whale is infinitesimal, but this is not the case. Mariners are well aware that collisions with ships are a major cause of whale mortality. Ship strikes fatal to whales were first recorded in the late 1800's as ships reached speeds of 13 – 15 knots, though they remained infrequent until the 1950's. As the number and speed of ships has increased, the occurrence has soared and it is now estimated that about 50% of the deaths of Northern Right whales in the Atlantic result from collisions [1]. In fact, the true occurrence may be even higher than that reported, because of the opprobrium associated with injuring or killing whales and the fact that, in the US, whales are afforded legal protection and collisions may result in litigation and heavy penalties. A secondary consideration in ship-whale collisions is the potential for damage to sonar equipment as many vessels have their sonar systems fitted to the bow or the keel, and one might also mention the prospect of human death and injury, as has been reported in collisions involving high speed ferries.

Concern about the frequency and consequences of ship strikes has led to proposals to reduce ship speeds to less than 10 knots in areas known to be frequented by whales, but this solution brings with it a high economic penalty and has other obvious drawbacks. A preferred approach is to avoid collisions by ship maneuver; this, of course, demands an effective ship-board whale detection capability. At present the principal means of detection is by visual observation from the bridge, but this approach is limited to day-time, is feasible only in low sea states, often has a restricted field of view, and relies on the human observer. A lot of research continues to focus on acoustic methods, but these, too, suffer from practical constraints. Active sonar cannot be used with high power as this injures the animals, and detection is further impaired by refraction effects. Passive sonar can detect whale sounds but obviously works only when whales are calling and is of limited utility on most ships because its performance degrades rapidly as speeds approach 15 knots. Thermal infrared optronic sensors are being explored but sensitivity is a critical issue as the external body temperature of whales at mid-latitudes is close to water temperature. The challenging possibility of detecting whale breath, which is warmer, has not been overlooked.

A candidate sensor which has received surprisingly scant attention, judging from the open literature, is ship-borne microwave radar, specifically X-band radar as this is fitted to the majority of ships, merchant and military. A study sponsored by the US Office of Naval Research, and led by Arete Associates, reported radar detections of breaching whales at ranges up to 8 km in low sea states (SS < 3), and of surfaced whales and dolphins at ranges up to 5 km [2], again in low sea states. These distances are compatible with the requirements of merchant ships which typically require at least 5 km to make a substantial manoeuver. The radar used in the ONR study was a standard Furuno X-band marine radar, which means that it employed horizontal polarisation for transmit and receive. Recent experiments with the DSTO Wandana fully polarimetric X-band radar have demonstrated very substantial improvements in discrete land target discrimination by means of filtering in the polarization domain [3]. This raises the possibility of a corresponding enhancement for marine mammal detection. In this paper we present some recent results of fully polarimetric radar measurements of cetaceans in the coastal waters south and east of Australia, and proceed to demonstrate that polarimetric filtering can indeed provide higher contrast and hence increase the probability of detection.

II. POLARIMETRIC RADAR

The defining attributes of polarimetric radar are (i) the transmission of signals in two independent (usually orthogonal) polarization states, and (ii) the coherent reception of the scattered electromagnetic field as projected onto two independent polarization states. The choice of basis for the polarization domain is in principle arbitrary but in practice usually confined to linear ('vertical' V and 'horizontal' H

978-1-4244-5222-4/10/$26.00 ©2010 CROWN

states), though left- and right-handed circular polarizations are sometimes used. The radar scattering properties of discrete, deterministic targets are adequately described by the familiar polarisation scattering matrix which relates the scattered field at the target to the incident field,

$$\begin{bmatrix} E_\eta^{scat} \\ E_\chi^{scat} \end{bmatrix} = \begin{bmatrix} S_{\eta\eta} & S_{\eta\chi} \\ S_{\chi\eta} & S_{\chi\chi} \end{bmatrix} \begin{bmatrix} E_\eta^{inc} \\ E_\chi^{inc} \end{bmatrix} \quad (1)$$

or, equivalently,

$$\vec{E}^{scat} = \tilde{S}\vec{E}^{inc} \quad (2)$$

where η and χ index a basis for the polarisation state of the electromagnetic field and $S_{\mu\nu} \in C, \mu, \nu = \{\eta, \chi\}$. The need to define a consistent coordinate system for the full radar measurement process can be satisfied by adopting either the forward scattering alignment convention for which the associated $\tilde{S}$ is termed the Jones matrix, or the backscatter alignment convention for which the associated $\tilde{S}$ is termed the Sinclair matrix.

III. Statistical polarimetry

In the deterministic scattering case, the scattering matrix represents a point-to-point mapping on the Poincaré sphere. When we encounter scattering from a random surface, each single radar observation of a given resolution cell is related to the incident field by a scattering matrix as before, but both the time series of observations from that cell, and the set of observations from all resolution cells at any one time, are random processes and must be described statistically. The randomness can be thought of as the consequence of the coherent addition of contributions from a host of small "scattering centres" disposed within the resolution cell. The scattered field is in general partially polarised because the fluctuating scattering centres do not share the same polarisation transformation properties.

Second-order moments of the probability distributions of the resultant scattered field are widely used to represent this stochastic behaviour, albeit incompletely. Those correlations which survive the averaging incurred in evaluating the moments embody the principal scattering mechanisms responsible for the observed scattering properties.

The group of all 2 × 2 matrices over C is isomorphic to a linear space Λ, so we can express $\tilde{S}$ in terms of a linear combination of basis elements for any basis we choose for Λ. For instance, the Pauli basis is attractive because its elements correspond to scattering matrices which embody simple, physically intuitive polarisation transformations, as manifested by canonical scatterers such as planes, dipoles and dihedrals. The vector of coefficients of this expansion, k, is thus an alternate representation of $\tilde{S}$. Moreover, rather than compute the required second-order moments directly from the scattered field components

$$\tilde{S}_{\eta\chi}\vec{E}_\chi \equiv \sum_\chi \tilde{S}_{\eta\chi}\vec{E}_\chi \quad (3)$$

it is advantageous to compute them from the bilinear products of the field combinations corresponding to the Pauli basis representation. We do this by evaluating the expectation value of the outer product $\langle k \otimes k^* \rangle$, the coherency matrix, where the expectation value is approximated by averaging over a number of contiguous spatial and temporal samples. For the monostatic scattering geometry case of interest here, symmetry dictates that the coherency matrix is of rank 3. This approach offers a deeper insight into the identities and relative strengths of the scattering mechanisms contributing to any given measurement.

As originally shown by Cloude and Pottier [4], information about the scattering mechanisms can be extracted by eigenanalysis of the coherency matrix and evaluation of functions of the eigenvalues λ_i :

(i) the entropy

$$H = -\sum_i p_i \log_3 p_i \quad (4)$$

where

$$p_i = \frac{\lambda_i}{\sum_n \lambda_n} \quad (5)$$

(ii) the anisotropy,

$$A = \frac{\lambda_2 - \lambda_3}{\lambda_2 + \lambda_3} \quad (6)$$

(iii) the $\bar{\alpha}$ - angle,

$$\bar{\alpha} = \sum_i p_i \alpha_i \quad (7)$$

where the α_i are obtained from the canonical transformations needed to diagonalise the coherency matrix.

The entropy and anisotropy are indicative of the number and relative strengths of mechanisms active, the $\bar{\alpha}$ - angle the type of scattering involved. These functions have been used extensively to classify SAR imagery. Their values can be thought of as the coordinates which define a three-dimensional vector space – the statistical polarimetry domain – though we often confine our attention to the entropy - $\bar{\alpha}$ subspace.

IV. Detection via Statistical polarimetric filters

It is often the case that one seeks to detect targets in the presence of sea clutter. With a single-polarisation radar, this objective is usually pursued by characterising the amplitude probability distribution of the clutter and using statistical decision theory to determine a detection threshold according to some criterion, such as limiting the probability of false alarm. When we have access to polarimetric information, we can exploit the additional signal dimensionality to define decision boundaries, not just for classification but for detection.

When dealing with a purely deterministic, known target, the detection problem admits a number of approaches based on optimal polarisations [5]. For example, knowing the target scattering matrix, one can maximise the target return by incident polarisation synthesis. Alternatively, or in addition, one can attempt to minimise the clutter power contribution by constructing a polarisation null on the reception Poincare sphere. In the case of concern in this paper, these approaches are not applicable, since the target is itself an unknown stochastic scatterer because of its structural complexity and fluctuating dynamics. Both clutter and target echoes are now described by probability distributions in the vector space used to represent the scattering behaviour. Importantly, just as it is advantageous with single polarisation radars to adapt radar parameters so as to maximise the signal-to-clutter ratio (SCR), so with polarimetric radars it would appear advantageous to adapt the radar parameters so as to maximise the separation of the statistical distributions corresponding respectively to target returns and clutter. In the context of classification, this may be seen as a form of polarimetric contrast enhancement [6].

In our previous studies of statistical polarimetric filtering we developed heuristic bilinear filters where the factors were the raw H-α-A values or their complements as defined by the range of possible values. Here we apply the same techniques to the whale detection problem and then examine an adaptive approach based on contrast enhancement.

V. The Great Australian Bight experiment

Australia is the winter home to around 1,500 of the 12,000 or so Southern Right Whales remaining worldwide, a small fraction of the estimated 60,000 - 100,000 that existed prior to whaling. The Head of Bight is a critical gathering area for Southern Right Whales with up to half of the Australian population using the area to calve, mate and socialise. They arrive in May and depart around October, spending the rest of the year feeding far offshore in the Southern Ocean. Each year between 25 and 55 calves are born at or near the Head of Bight, making it one of the three largest breeding areas along the Australian coast.

Much of the Bight lies due south of the Nullarbor Plain, which meets the Southern Ocean in stunning cliffs (up to 95 m high) which provide an excellent location for land-based observations of whales and dolphins. The measurements reported here were taken at a location approximately 90 km west of the Nullarbor roadhouse where the cliffs are the highest, and where the bathymetry results in a low reflection wave coefficient. This region falls within the Yalata Indigenous Protected Area. The measurement location is indicated in Figure 1.

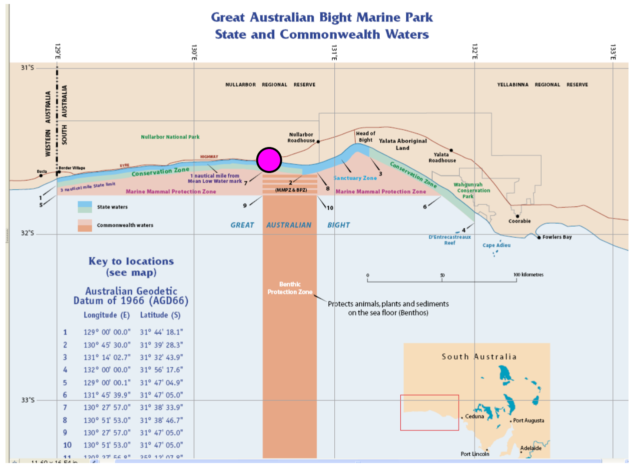

Figure 1. The location of the whale measurements, indicated by the magenta disc.

The measurements reported here were carried out at X-band, since this is the frequency band in most common use in commercial and naval ship radars. Unlike those radars, though, the DSTO Wandana mobile radar is coherent and fully polarimetric, working in the linear basis, with a waveform repetition frequency of 50 Hz, alternating between H- and V-polarisations. For the whale measurements, the radar used a step-frequency waveform with 1024 steps of 0.5 MHz to yield an effective range resolution of 0.3 m. A pulse width of 2 microseconds was employed to provide a 300 m footprint within which the high range resolution analysis was performed. The azimuthal beamwidth of the antenna is 4° so the cross-range dimension of a resolution cell at 300 m range is 20 m. This is not an issue here, though, as the statistical polarimetric decomposition requires averaging over a number of range-time cells, for which the range dimension is admirably suited. The radar was positioned on a cliff top son that measurements could be made over a wide range of incidence angles, noting that the application to ship-borne radars places most emphasis on angles close to grazing. Figure 2 shows the radar van in position during measurements, while Figure 3 shows a female Southern Right whale just breaking the surface.

VI. Processing

The received signals were range-processed and combined to form an estimate for the Pauli scattering vector for each range-time cell. The 3 x 3 polarimetric coherency matrices were then formed from the outer product of the Pauli scattering vector averaged over a 1 x 15 cell. Next, an eigenvalue decomposition was performed and the polarimetric entropy, anisotropy and mean scattering alpha values determined for each cell. These raw estimates were then combined in bilinear products as potential feature spaces for detection, used to synthesise the response to circularly-polarised radar signals and also used as input to the exploratory adaptive training procedures.

Figure 2. The radar van in position at the edge of the cliff, overlooking the waters where the whales congregate

Figure 3. A female Southern Right whale photographed from the radar site

VII. RESULTS

A representative episode when a single whale traversed the illuminated footprint is shown in Figure 4. The images have axes of range and time, with the colour-coded variables being the squared magnitudes of the HH, VV and HV (= VH) elements of the scattering matrix. In all the figures shown here, the patch of sea illuminated by the radar beam is narrower than the processed range depth, so the extremities of the range domain are not illuminated. Further, the beam was adjusted during the experiment to keep the whale in the beam.

We see immediately that the whale track is evident in all three but in the VV case is heavily masked by sea clutter. Further, all three components show the presence of oblique lines, corresponding to ambient sea waves with a (radial) speed of about 7.9 ms^{-1}. The period of the waves, as determined from the images, is about 15 s, for which the wave celerity is predicted to be 23.4 ms^{-1} and the group velocity half that, ~ 11.7 ms^{-1}. These values yield an estimate of the angle between the radar look direction and the direction of wave propagation,

$$\varphi \approx \cos^{-1}\left(\frac{7.9}{11.7}\right) \approx 48^\circ \qquad (8)$$

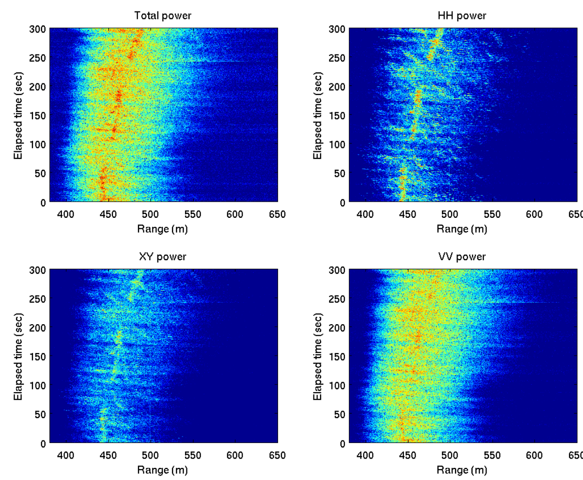

Figure 4. Range-time map of the squared magnitude of the elements of the scattering matrix during the transit of a single whale, evaluated in the linear H-V basis

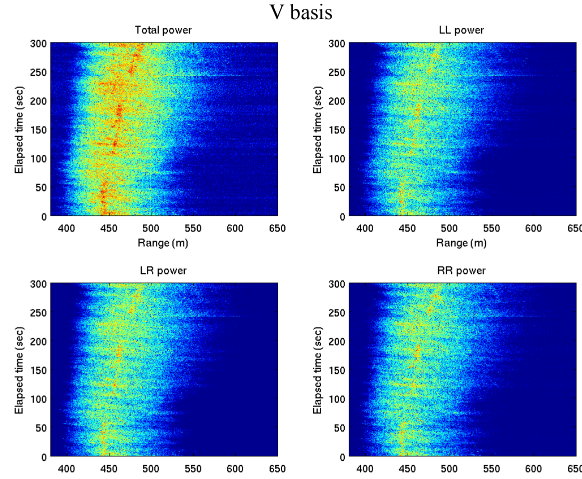

Figure 5. As for Figure 4 but evaluated in the LCP-RCP circular polarization basis

At the time the radar look direction was ~ 170° and the swell was judged to arrive from ~ 225°, so the observed angle with respect to the radar look axis was ~ 55°, in good agreement with measurement.

As we are in possession of the full scattering matrix, it is an easy matter to synthesise the sea response to other incident polarizations. To illustrate, Figure 5 shows the squared magnitudes for circular polarizations. The striking difference between Figures 4 and 5 is the much higher discrimination of the whale track in Figure 4.

Though the magnitudes of the matrix elements for circular polarizations are comparable, the inter-element coherence exhibits high coupling between co-pol and cross-pol terms for sea clutter but extremely low values for the resolution cells containing the whale (Figure 6c,d). As a consequence, the whale track is strongly enhanced in this domain. This is not the case for the coupling between the two orthogonal co-pol channels (Figure 6b).

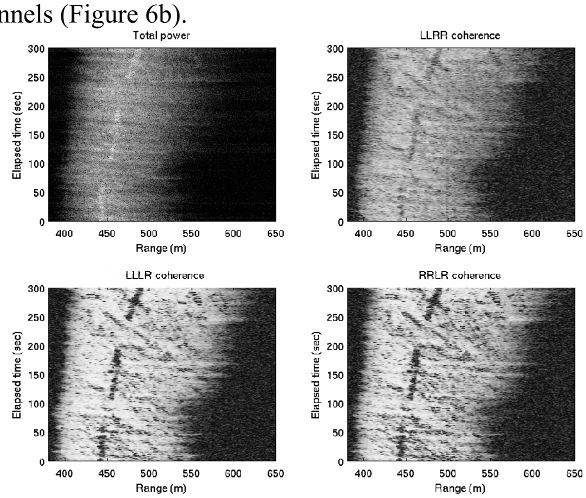

Figure 6. Range-time map of the measured coherence between various states in the circular polarization basis

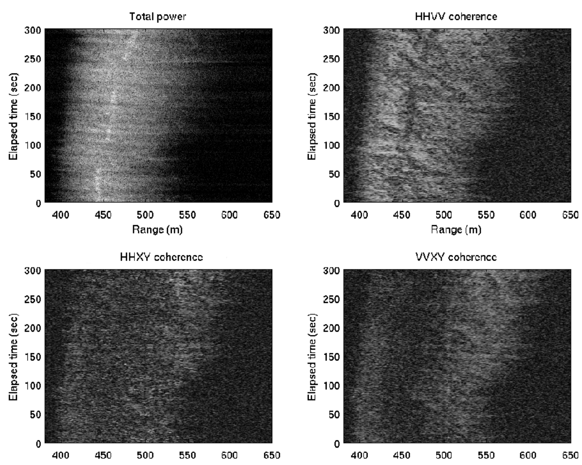

Figure 7. As for Figure 6 but in the linear H-V basis

The linear polarization basis yields low to moderate values for all cells, as shown in Figure 7, and hence the coherence offers no guide to filter design.

Turning to the statistical measures, Figure 8 presents the Cloude-Pottier analysis of the same data. Here we can see the whale track characterized by an entropy value somewhat below that of highly disturbed surfaces or areas of significant microscale wave breaking seen elsewhere in the image, such as along wave crests. Consistent with this, there is a slight reduction in the α value and a moderate anisotropy, together indicative of new geometrical features on the surface. Though these may be small, they clearly have an appreciable effect on the active scattering mechanisms.

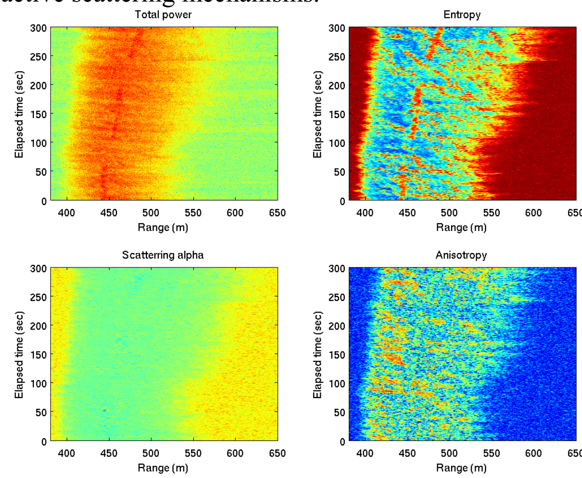

Figure 8. Range-time map of the alpha-entropy-anisotropy decomposition parameters

The bilinear filter used in a previous (land-based) application employed products of the basic variables. Figure 9 is a compilation of the resulting features.

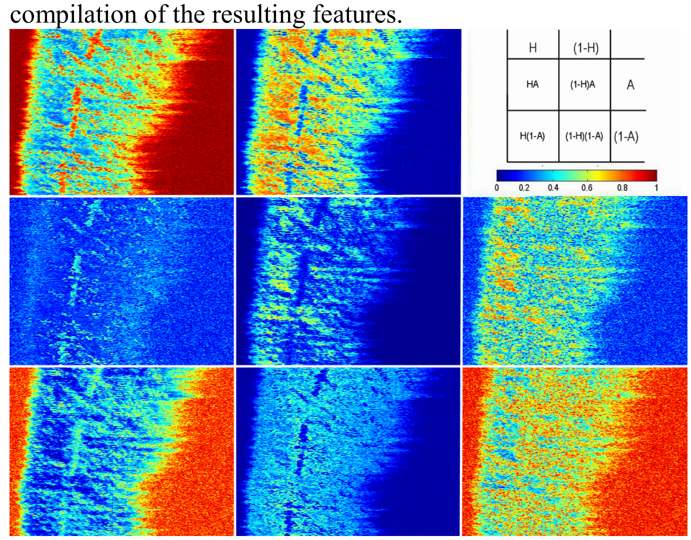

Figure 9. Bilinear products of entropy-anisotropy parameters as used to implement polarimetric filtering for feature enhancement

From an inspection of these alternative representations of the polarimetric characteristics of the scattered fields, it is apparent that the contrast of the whale track against the clutter background varies dramatically from one representation to another. Moreover, concentrating for the moment on just two bases – linear and circular – a comparison of Figures 4 and 5 demonstrates that the linear basis provides the better contrast in terms of scattering matrix elements, while Figures 6 and 7 demonstrate that the circular basis yields far better discrimination in terms of inter-channel coherence.

VIII. TOWARDS AN OPTIMAL DETECTION SCHEME

The most obvious approach to whale detection is to employ one of the two or three representation spaces which worked well in the case presented. For instance, the LLLR inter-element coherence in the circular basis is an obvious candidate. Yet no claim can be made that this choice is optimal. A preferred approach would be to formulate the detection problem as an optimization procedure, using a suitable contrast metric. This can be done in a number of ways, but here we propose the following.

Suppose we have the scattering matrices of all the resolution cells in a basis $\{\eta, \chi\}$. By means of a unitary transformation $U_{\eta\chi}^{\kappa\lambda}$ we can transform these scattering matrices to a new basis, $\{\kappa, \lambda\}$,

$$S_{\kappa\lambda} = U_{\eta\chi}^{\kappa\lambda\,H} S_{\eta\chi} U_{\eta\chi}^{\kappa\lambda} \tag{9}$$

The quantity that we wish to maximize is the contrast between cells containing a whale and cells with only sea present. Rather than deal with individual spatial cells, we shall work with a localized patch in the range-time domain, so that statistical averaging can be exploited to produce a robust discrimination function. For instance, we might allow for 20 m in range to allow for the case of a whale aligned along the radar axis, and assume, on the basis of observations, that a typical radial speed component is 0.4 ms^{-1}, giving us a patch duration of 50 s. This gives us a rectangular box $A(r_i, t_j)$ centered on the test cell (r_i, t_j) for the "signal". The contrast is to be achieved against the neighboring background, so we take two regions, B_{low} and B_{high}, one on each side of the "signal patch under test" in the range dimension and extending over the same time interval. The measure of contrast is chosen to be of the form

$$\Phi(r_i, t_j) = \frac{\Xi(A(r_i, t_j))}{\sqrt{\Xi(B_{low})\Xi(B_{high})}} \tag{10}$$

where the function Ξ (which is normalized to unit area in the range-time domain), is yet to be assigned. The key point is that Ξ is dependent on the polarization basis, $\Xi(X) \equiv \Xi(X; \mu, \nu)$. The optimization problem can now be formulated in terms of the measure Φ defined on the Poincare sphere : find the basis $\{\mu, \nu\}$ for which $\Phi[\Xi(X; \mu, \nu)]$ is the desired extremum. (Clearly it is sufficient to define only one basis vector as the orthogonal state lies at the antipode.)

We illustrate this procedure by setting Ξ as follows :

$$\Xi(X; \mu, \nu) = (\zeta(X))^{-1} . \sum_{(r_i, t_j) \in X} \left| S_{\mu\mu}(r_i, t_j) \right|^2 \tag{11}$$

where $\zeta(X)$ is the area of X in the range-time domain.

This function is shown evaluated on the Poincare sphere in Figure 10, indicating the extremum. Not surprisingly, it lies close to the H-polarisation state, consistent with the data plotted in Figure 4.

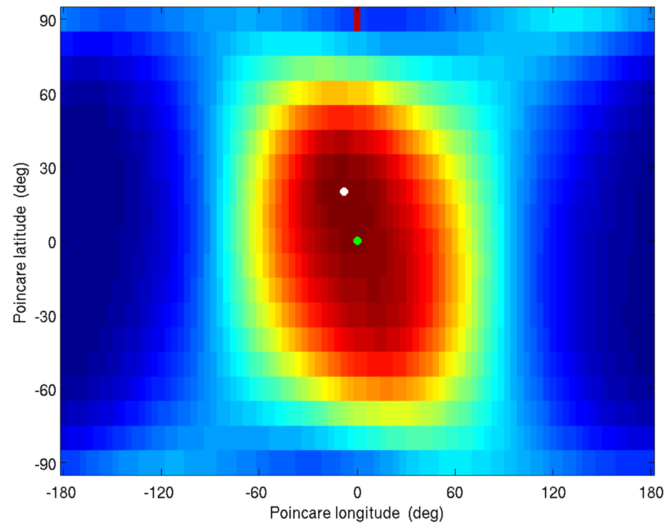

Figure 10. Contrast function as defined by (11); green marker corresponds to HH polarization, white marker is extremum

IX. CONCLUSION

In this paper we have shown how the polarization domain provides many options for representing scattered field information. The utility of this in the whale detection context is the fact that some representations yield enhanced contrast between cells containing whales and those containing only sea. We have demonstrated this with several different representations and outlined an approach for finding the optimum detector given a sample with a whale present. The next phase of this research will be to characterize the scattering mechanisms involved so that no training sequence is required.

X. REFERENCES

[1] 'Large Whale Ship Strikes Relative to Vessel Speed', NOAA report www.nero.noaa.gov/shipstrike/.../white_paper_Speed_18Aug_2004.pdf

[2] D.F. DeProspo, J. Mobley, W. Hom, and M. Carron, "Radar-based detection, tracking and speciation of marine mammals from ships", Arete Associates Project Report, 2004

[3] J.T. Morris, W.C. Anderson, and S.J. Anderson, "Polarisation filtering for small target discrimination in ground clutter", Proceedings of the IEEE International Radar Conference, *Radar 2007*, Edinburgh, October 2007

[4] E. Pottier, and S.R.Cloude, 'A review of target decomposition theorems in radar polarimetry', IEEE Trans. Geoscience and Remore Sensing, vol.34, no.2, pp.498-518, March 1996

[5] J.R. Huynen, 'Phenomenological theory of radar targets', Ph. D. thesis, Technical Univ., Delft, Netherlands, 1970

[6] H. Mott, 'Remote sensing with polarimetric radar', Wiley 2007,